







## Article

# Otolith Morphometric and Shape Distinction of Three Redfin Species under the Genus *Decapterus* (Teleostei: Carangidae) from Sulu Sea, Philippines

Christian James C. Morales <sup>1,\*</sup>, Kyle Dominic E. Barnuevo <sup>2</sup>, Emmanuel S. Delloro, Jr. <sup>1,3</sup>, Roxanne A. Cabebe-Barnuevo <sup>1,3</sup>, Jenylle Kate S. Calizo <sup>2</sup>, Sanny David P. Lumayno <sup>2</sup> and Ricardo P. Babaran <sup>1</sup>

- <sup>1</sup> Institute of Marine Fisheries and Oceanology, College of Fisheries and Ocean Sciences, University of the Philippines Visayas, Miagao, Iloilo 5023, Philippines
- <sup>2</sup> Institute of Aquaculture, College of Fisheries and Ocean Sciences, University of the Philippines Visayas, Miagao, Iloilo 5023, Philippines
- <sup>3</sup> Department of Science and Technology, Science Education Institute, DOST Compound, Bicutan, Taguig City 1631, Philippines
- \* Correspondence: ccmorales2@up.edu.ph

**Abstract:** Otoliths are paired calcified structures in the inner ear of teleosts that function in hearing and balance. In this study, the use of otolith morphometrics and shape analysis were explored to delineate the redfin species under the genus *Decapterus* from the Sulu Sea, Philippines, namely, *Decapterus kurroides*, *D. smithvanizi*, and *D. tabl*. Results showed that the mean otolith shapes are unique within species ( $p < 0.001$ ). The otolith size-related (OW—otolith weight, OL—otolith length, OH—otolith height, OA—otolith area, and OP—otolith perimeter) and shape-related (RE—rectangularity, SQ—squareness, EL—ellipticity, RO—roundness, AR—aspect ratio, FF—form factor, CO—compactness, and CI—circularity) morphometric indices also showed significant variations ( $p < 0.001$ ) among the three species. Distinct regions differentiating *D. kurroides* from the other two species were seen along the dorsal margin of the otoliths, which was supported by its significantly higher values for OH (size-related index) and RO (shape-related index). In addition, the morphometric indices showed significant variations ( $p < 0.001$ ), except for RE. Furthermore, it was revealed that the size-related indices were able to separate *D. kurroides* from the other two species, which turned out to be indifferent. The results provided relevant data on the use of otoliths as an additional confirmatory tool in species delineation of the identified redfin species, and, therefore, offer opportunities of applying the same method in delineation and, eventually, identification of species from other genera, especially those that closely resemble each other.

**Keywords:** *Decapterus kurroides*; *Decapterus smithvanizi*; *Decapterus tabl*; small pelagics; species delineation; taxonomy



**Citation:** Morales, C.J.C.; Barnuevo, K.D.E.; Delloro, E.S., Jr.; Cabebe-Barnuevo, R.A.; Calizo, J.K.S.; Lumayno, S.D.P.; Babaran, R.P. Otolith Morphometric and Shape Distinction of Three Redfin Species under the Genus *Decapterus* (Teleostei: Carangidae) from Sulu Sea, Philippines. *Fishes* **2023**, *8*, 95. <https://doi.org/10.3390/fishes8020095>

Academic Editors: Josipa Ferri and Wann-Nian Tzeng

Received: 26 December 2022

Revised: 30 January 2023

Accepted: 30 January 2023

Published: 5 February 2023



**Copyright:** © 2023 by the authors. Licensee MDPI, Basel, Switzerland. This article is an open access article distributed under the terms and conditions of the Creative Commons Attribution (CC BY) license (<https://creativecommons.org/licenses/by/4.0/>).

## 1. Introduction

Otoliths are structures that can be found in the inner ear of Teleost fishes that mainly function in hearing and balance [1]. These are made of calcium carbonate and contain small amounts of proteinaceous matter [2]. As the fish grows, new calcium carbonate layers deposit onto the otolith surface. Otoliths are important in studies on fish populations and stocks by being valuable natural tags because of their continuous growth and metabolic inertness. Information that the otolith contains can be used to indicate ecosystem range, spatial distribution, and stock structure of fish species [3]. Otolith shape and chemistry, on the other hand, are among the methods used in stock delineation. They can be simple to technical, quantitative, and sophisticated. Some examples include catch data, mark-recapture experiments and molecular methods [4,5], parasite incidence [6,7], scale and otolith microchemistry, stable isotopes, shape, microstructure [8–11], and life history [12].

Otoliths can have unique shapes that correspond to species [13,14] but intraspecific variations may exist [15,16]. Some studies also showed directional (ear-side) and ontogenetic asymmetry in the same species [17–22]. Fish with different life histories often show differences in otolith morphology as a collective result of genetics and environment [23]. In addition, otolith shapes may vary geographically relative to environmental factors as well as fish growth [22,24–26]. Berg et al. [27] highlighted the strong effects of genetic factors, while some underlined the effects of environmental parameters, such as temperature, depth, salinity, substrate, and feeding conditions [28–31]. Genetically-induced changes become more pronounced since the environment alters otolith growth rate, which then modifies the shape of the otolith [25,27,32].

The archipelagic waters of the Philippines are home to a wide variety of marine resources that serve as a viable source of food and livelihood in the form of multi-scale, multi-gear, and open access multispecies exploitation. This supports about 70% of Filipinos that live in coastal areas [33]. Among the most harvested resources (in volume) are small pelagic fishes that make up the top numbers in annual municipal and commercial capture fisheries production (see PSA [34]). One of the most important small pelagic fishes in the country are the *Decapterus* species., locally known as “galunggong” or roundscads. This group is characterized by a single finlet posterior to both the second dorsal and anal fins and lack scutes on the anterior curved part of the lateral line [35]. There are currently 11 valid species listed under the genus [35,36]. The redfin *Decapterus* group, which was clustered by Kimura et al. [35], includes *Decapterus akaadsi* Abe, 1958; *D. kurroides* Bleeker, 1855; *D. smithvanizi* Kimura, Katahira and Kuriwa, 2013; and *D. tabl* Berry, 1968. The different species of redfin *Decapterus* were all reported in the Philippines: *D. kurroides* by Kimura et al. [35]; *D. tabl* by Narido et al. [37], Kimura [38], and Motomura et al. [39]; *D. akaadsi* by Smith-Vaniz et al. [40]; and the most recent report, *D. smithvanizi*, by Delloro et al. [41] in Panay Island, Philippines. The redfin group is collectively known as “pula-ikog”, most particularly in Panay Island. At present, studies on the redfin group are very few and almost limited to records of existence and taxonomic descriptions. These studies mostly relied on the use of morphometrics, meristics, and genetic differentiation. Visually, there can be very little and very intricate differences among the three recorded species (*D. kurroides*, *D. smithvanizi*, and *D. tabl*). Some of the most prominent descriptors listed by Delloro et al. [41] include the deeper body of *D. kurroides*, compared to the slender *D. smithvanizi* and *D. tabl*, which is also shown in Figure 1. Furthermore, the length of the pectoral fin is shorter in *D. tabl* than in *D. smithvanizi*.

Due to the strong resemblance of *D. kurroides*, *D. smithvanizi*, and *D. tabl* with each other, the three redfin *Decapterus* species are categorized as one by fishers (even hired enumerators) from Panay Island, Philippines, in fish landings and markets. For this reason, they are being reported as a single species or generalized as “galunggong” or roundscads in fisheries assessments and landed catch enumeration that form local and national fisheries statistics. To address this issue, the morphometrics and shape of the right sagittal otoliths were investigated by creating a valid representation of the mean otolith morphometric observations and shape outlines. Otolith size and shape relationships with fish length were also examined. The purpose of this study was to investigate the main hypothesis that the three redfin *Decapterus* species from the Sulu Sea, Philippines, may be identified and distinguished from one another using otoliths.



**Figure 1.** Representative images of the three redfin *Decapterus* species used in this study: (A) *Decapterus kurroides*; (B) *D. smithvanizi*; (C) *D. tabl*. Photos by E.S.D.J.

## 2. Materials and Methods

### 2.1. Sample Collection

Non-live fresh samples of *Decapterus kurroides*, *D. smithvanizi*, and *D. tabl* were purchased from fish markets in the province of Iloilo, Philippines, namely, San Joaquin, Miagao, and Guimbal (see Figure 2). Samples were from the adjacent Sulu Sea, which is the most prominent fishing ground in the area. This information was based on preliminary surveys conducted on fishers that operate commercial fishing vessels from the landing sites. A total

of 82 redfin specimens were collected from February to July 2021. Upon transport to the laboratory, the standard length (SL) and total length (TL) were measured to the nearest 0.1 cm using a digital caliper (Mitutoyo ABSOLUTE Series 500), while the total weight (BW) was taken in 0.1 g using a digital weighing scale. Species identification followed Motomura et al. [39] and Delloro et al. [41]. The *D. kurroides* samples had TL ranging from 15.2 to 27.3 cm. For *D. smithvanizi* and *D. tabl*, the samples' TL range were 13.9–21.8 cm and 18.3–25.4 cm, respectively. These results are summarized in Table 1.

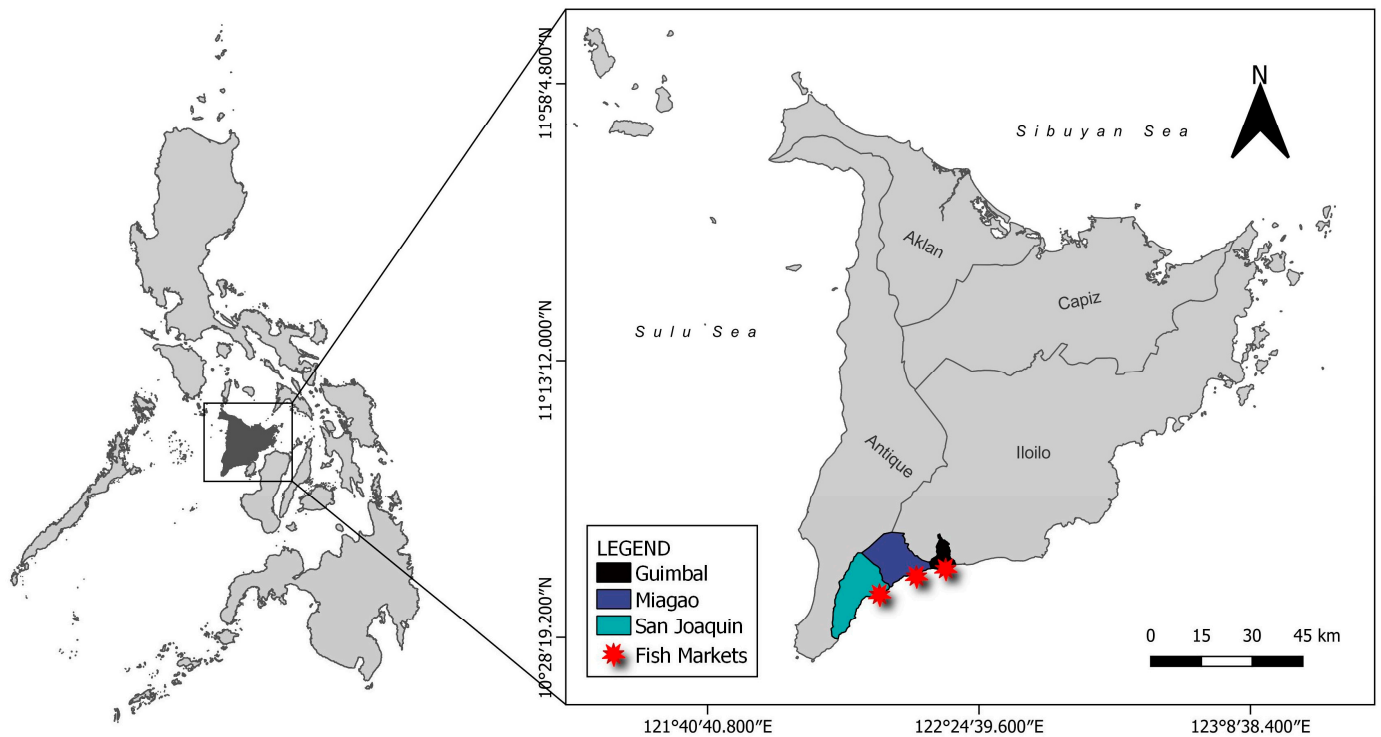


**Figure 2.** Map showing Panay Island and the location of fish markets in the province of Iloilo where fish samples were collected.

**Table 1.** Summary of length and weight of redfin *Decapterus* from the Sulu Sea used in this study.

Species	N	Mean Body Weight (g) ± SD	Mean Total Length (cm) ± SD
<i>Decapterus kurroides</i>	32	115.853 ± 85.14	20.222 ± 4.90
<i>Decapterus smithvanizi</i>	34	59.682 ± 19.11	17.844 ± 1.86
<i>Decapterus tabl</i>	16	100.925 ± 29.42	21.863 ± 2.22

## 2.2. Otolith Extraction and Storage

Consistent with the methods in Barnuevo et al. [16], the sagittal otoliths were extracted from the samples, first, by locating the otic capsule in the post-ventral portion of the neurocranium. A shallow incision was created in the middle portion of the otic capsule, which eventually gently broke, and the sagittal otoliths were exposed and extracted using fine forceps. The collected otoliths were pre-cleaned with distilled water, submerged in bleach for 20 to 30 s to remove remaining blood and muscle debris, and immersed in absolute ethanol until air-dried. The samples were stored in 2.5 mL Eppendorf microcentrifuge tubes. The weights of individual otoliths (OW) were measured using a Shimadzu ATX224 analytical balance (Shimadzu Corporation, Kyoto, Japan; precision: 0.1 mg).

## 2.3. Sample Imaging

Each otolith used in this study was photographed using an Olympus SZ61 stereomicroscope (Evident Corporation, Tokyo, Japan) with an XCAM 1080PHB c-mount camera

(ToupTek Photonics, Hangzhou, China). The samples were laid on the non-sulcus side. Imaging was guided with a ruler for calibration and reference for the proceeding measurements. A total of 32, 34, and 16 right otoliths were imaged, representing *D. kurroides*, *D. smithvanizi*, and *D. tabl*, respectively.

#### 2.4. Otolith Morphometry

Five indices related to otolith size were obtained: otolith weight (OW), otolith length (OL), otolith height (OH), otolith area (OA), and otolith perimeter (OP), which were measured in ImageJ (NIH, USA). Furthermore, eight shape indices were calculated: rectangularity (RE), squareness (SQ), ellipticity (EL), roundness (RO), aspect ratio (AR), form factor (FF), compactness (CO), and circularity (CI) using the equations provided by Osman et al. [42].

#### 2.5. Otolith Shape Analysis

To visualize the differences in the otolith shape of three identified redfin species, images were subjected to shape analysis using the ShapeR 0.1–5 package [43] in Rstudio version 4.1.1 [44] to generate Wavelet coefficients. Additional packages used were Vegan 2.6–4 [45] and ggplot2 3.3.3 [46] for creating high resolution plots. Due to the difficulties encountered in detecting the outlines from raw otolith images, even when increasing the “detect.outline” threshold (0.1–0.5), the otolith images were converted into black and white using an image editing software (see Figure 3). This added step increased the detectability of the otolith outlines (at threshold = 0.1–0.2), as the possible effects of glares on the otolith surface were eliminated.

#### 2.6. Data Analyses

A cross-correlation analysis between fish length and raw measured data on otolith size indices was performed in jamovi version 2.3.18 [47] using the “Regression” module to show the relationships between fish size and the descriptors and between each other. Since we observed that the otolith morphometric indices are highly correlated with fish total length, we perceived the need to remove the allometric influence to the indices. Without allometry correction, it would be difficult to say that the morphometric and shape differences in otoliths are indeed interspecific differences within the *Decapterus* group rather than just differences implicated by collecting different sizes of fish.

To remove allometric influence and enable unbiased statistical observations, the otolith size indices were scaled up with the TL of fish using linear regressions [48,49]. The slope ( $b$ ) from the linear regressions were calculated and were used to remove allometric influence on data. The formula  $M_s = M_o(\bar{x}/x)^b$  followed Deepa et al. [50] (based on original equation by Lleonart et al. [51]), where  $M_s$  is the allometry-corrected measurement;  $M_o$  is the original otolith size parameter;  $\bar{x}$  is the mean size parameter for all specimens;  $x$  is the size parameter of each specimen; and  $b$  is the slope of the regression between  $\log M_o$  and  $\log(x)$  [45,51,52]. The equation was applied to both size-related and shape-related indices. The resulting values were used in the proceeding analyses.

The allometry-corrected data were tested using the Shapiro–Wilk test for normality. Results have shown that the data is not normally distributed ( $p < 0.001$ ). Hence, to compare the differences in the allometry-corrected morphometric measurements of the otoliths between species as well as the OL/TL and OH/OL proportions, non-parametric analysis of variance (Kruskal–Wallis) was performed in jamovi using the “ANOVA” module. Along with the Kruskal–Wallis test was Dwass–Steel–Critchlow–Fligner (DSCF) pairwise comparison for the post-hoc test. Furthermore, to characterize and visualize the influences and differentiation of each species based on allometry-corrected otolith morphometric measurements by the dimension reduction procedure, a principal component analysis (PCA) was performed in RStudio version 4.1.1.

The mean shape of the otoliths from the three redfin species under the genus *Decapterus* were obtained using the ShapeR and Vegan packages in RStudio using the “detect.outline”

function and were plotted using the Wavelet coefficients. To further characterize the differences in mean otolith shapes between the three redfin species, an ANOVA-like permutation test (function in ShapeR) was also ran for both smoothed and non-smoothed outlines. To further support these results, a constrained ordination (Canonical Analysis of Principal Coordinates) was performed using the Wavelet coefficients, which were visualized using the ggplot2 package.

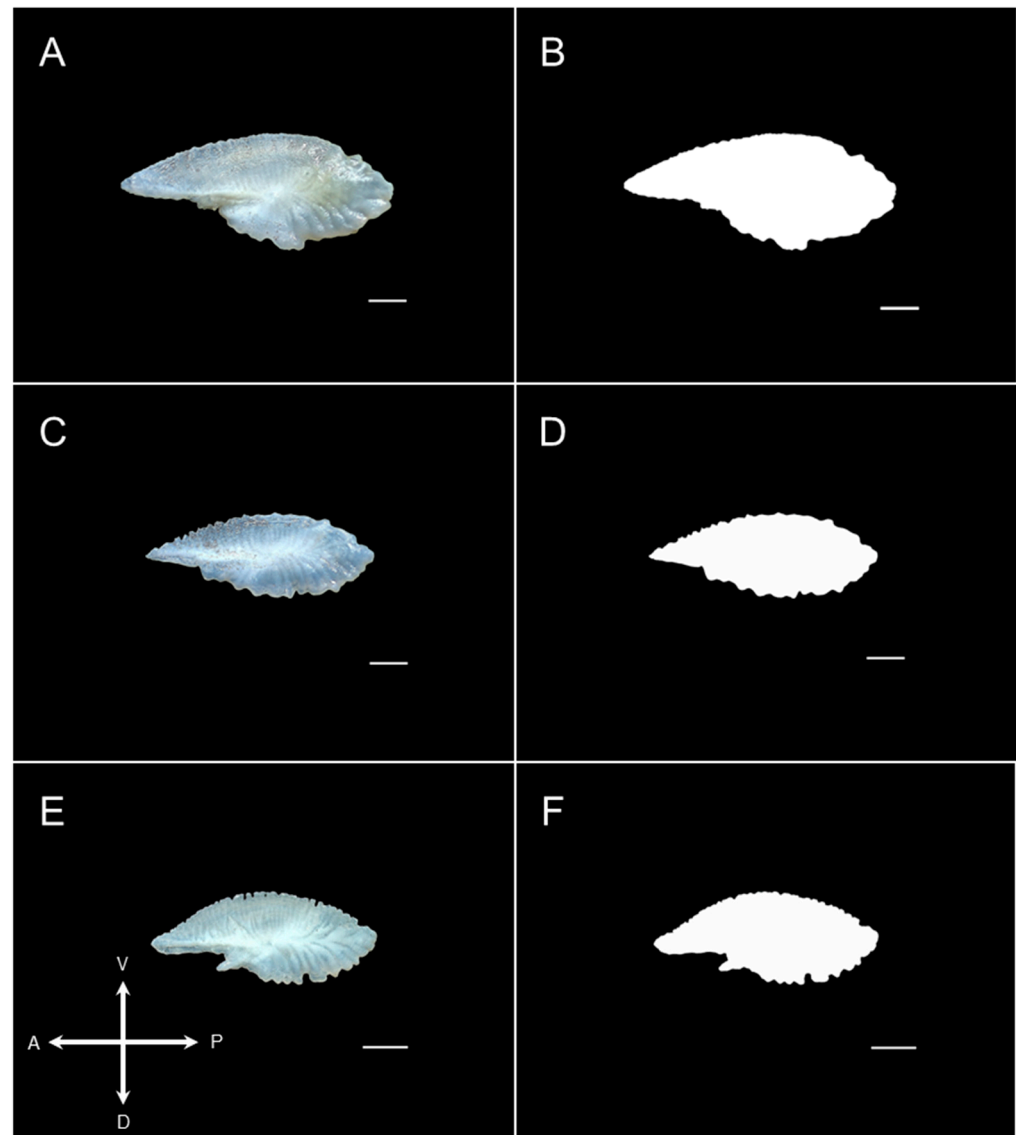


**Figure 3.** Raw and edited right sagittal otolith images of *Decapterus kurroides*—26.9 cm TL (A,B), *D. smithvanizi*—21.8 cm TL (C,D), and *D. tabl*—22.6 cm TL (E,F). The crossmap (lower-left) indicates the position of the otoliths: anterior (A); ventral (V); dorsal (D); posterior (P). Scale bar: 1 mm.

### 3. Results

#### 3.1. Otolith Morphometry

The group descriptives showed that *D. kurroides* had heavier ( $OW = 0.63 \pm 0.06$  mg), longer ( $OL = 5.41 \pm 0.17$  mm), and taller ( $OH = 2.44 \pm 0.10$  mm) otoliths that covered larger OA ( $8.30 \pm 0.46$  mm<sup>2</sup>) and OP ( $13.96 \pm 0.56$  mm) compared to the other two species. The mean values of OW, OL, OH, OA, and OP for *D. smithvanizi* were  $0.31 \pm 0.03$  mg,  $4.53 \pm 0.21$  mm,  $1.92 \pm 0.07$  mm,  $5.54 \pm 0.29$  mm<sup>2</sup>, and  $11.87 \pm 0.58$  mm, respectively. For *D. tabl*, mean values were  $0.39 \pm 0.07$  mg,  $4.10 \pm 0.71$  mm,  $1.73 \pm 0.29$  mm,  $4.53 \pm 1.41$  mm<sup>2</sup>, and  $11.10 \pm 2.11$  mm for OW, OL, OH, OA, and OP, respectively. In terms

of the shape-related indices, *D. kurroides* had the highest mean values for RO ( $0.36 \pm 0.02$ ) and FF ( $0.54 \pm 0.03$ ), indicating that its otoliths are significantly rounder and more irregular compared to the other two species ( $p < 0.001$ ). The highest mean values were also observed for RE ( $0.64 \pm 0.02$ ) and SQ ( $3.99 \pm 0.42$ ) in *D. smithvanizi*, which corresponds to greater variation in length and width with respect to OA. Finally, relative to the other two species, *D. tabl* otoliths were more elliptic ( $0.41 \pm 0.01$ ) to circular ( $0.66 \pm 0.38$ ), more compact ( $27.68 \pm 3.14$ ), and had higher AR ( $2.37 \pm 0.07$ ).

The summary of the calculated proportions of OL/TL and OH/OL are presented in Table 2. In *D. kurroides*, OL/TL was  $2.68 \pm 0.11\%$  (mean  $\pm$  SD), while, in *D. smithvanizi* and *D. tabl*, OL/TL were  $2.52 \pm 0.12\%$  and  $1.88 \pm 0.44\%$ , respectively. For OH/OL, values were  $45.46 \pm 3.34\%$  in *D. kurroides*,  $46.6 \pm 2.40\%$  in *D. smithvanizi*, and  $42.29 \pm 1.53\%$  in *D. tabl*. The Kruskal–Wallis test and DSCF pairwise comparison has further shown that the OL/TL proportions between species were significantly different ( $p < 0.001$ ), while, for OH/OL, the proportions were indifferent ( $p > 0.05$ ) between *D. smithvanizi* and *D. tabl*.

**Table 2.** Summary table of Kruskal–Wallis and DSCF pairwise comparison tests for the calculated proportions of OL/TL and OH/OL in the three redfin *Decapterus* species from the Sulu Sea.

OL/TL		$\chi^2$	df	W
<i>Decapterus kurroides</i>	<i>Decapterus smithvanizi</i>	53.0	2	−6.82 ***
<i>Decapterus kurroides</i>	<i>Decapterus tabl</i>		2	−7.92 ***
<i>Decapterus smithvanizi</i>	<i>Decapterus tabl</i>		2	−7.91 ***
OH/OL				
<i>Decapterus kurroides</i>	<i>Decapterus smithvanizi</i>	18.8	2	−5.262 ***
<i>Decapterus kurroides</i>	<i>Decapterus tabl</i>		2	−5.042 **
<i>Decapterus smithvanizi</i>	<i>Decapterus tabl</i>		2	−0.676

Note: \*\* =  $p < 0.01$ , \*\*\* =  $p < 0.001$ .

The Kruskal–Wallis test has also revealed that the allometry-corrected morphometric indices were generally distinct within species ( $p < 0.001$ ), except for RE ( $p > 0.05$ ). Post-hoc tests have further shown significant differences ( $p < 0.05$ ) between in the indices between *D. kurroides* and *D. smithvanizi*, except for RE ( $p > 0.05$ , Table 3). The same was observed for the comparison between *D. kurroides* and *D. tabl*. Finally, between *D. smithvanizi* and *D. tabl*, OL, OP, RE, EL, RO, and AR were indifferent ( $p > 0.05$ ).

Prior to the PCA, a Kaiser–Meyer–Olkin (KMO) test within the PCA of the “Factor” module in jamovi was performed. The overall result was a value of 0.74, which is classified as “middling” and was therefore accepted as an adequate sampling of the variables. Moving on, the results of the PCA showed that the PC2, which comprised the size- and shape-related indices (except for RE), explained 53.7% of the variation in the otoliths. The PC2, on the other hand, which included the size-related indices, OL, OA, OP, and all the shape-related indices (except SQ), explained the additional 21.9% of the variation. Together, they explained 75.6% of the variation in the otoliths of the three redfin *Decapterus* species.

Figure 4 shows the groupings of the three redfin *Decapterus* species based on the morphometric indices of their otoliths. The *D. kurroides* cluster was situated along the positive region of the PC1, while *D. smithvanizi* and *D. tabl* were along the negative region of the same axis. The biplot further shows how the variables in the PC1 were able to separate *D. kurroides* from the other two species as evidenced by its distance to the overlapping cluster, indicating otolith variables from *D. smithvanizi* and *D. tabl*. The PC2, conversely, has shown that there is little to no difference between *D. kurroides*, *D. smithvanizi*, and *D. tabl*. The differences in the values of size- and shape-related indices can also be seen in the directions of the vectors that represent variable loadings. From this data, we infer that the size-related indices, OW, OL, OH, OA, and OP can separate *D. kurroides* from the other two species. For the shape-related indices, *D. smithvanizi* and *D. tabl* shared similar values for EL, AR, and CO and, hence, cannot be used as indicators of their distinction. Moreover, RE,

RO, and FF did not belong to any of the clusters. Hence, they cannot be used to separate the three redfin *Decapterus* species.

**Table 3.** Summary table for Kruskal–Wallis test using the size- and shape-related morphometric Indices from the three redfin *Decapterus* species from the Sulu Sea, Philippines.

		$\chi^2$	df	$\epsilon^2$
Size-related indices	OW	65.75 ***	2	0.81
	OL	56.35 ***	2	0.70
	OH	60.67 ***	2	0.75
	OA	60.96 ***	2	0.75
	OP	52.61 ***	2	0.65
Shape-related indices	RE	3.36	2	0.04
	SQ	58.83 ***	2	0.73
	EL	26.99 ***	2	0.33
	RO	18.60 ***	2	0.23
	AR	25.70 ***	2	0.32
	FF	33.39 ***	2	0.41
	CO	33.39 ***	2	0.41
	CI	63.26 ***	2	0.78

Note: \*\*\* =  $p < 0.001$ .

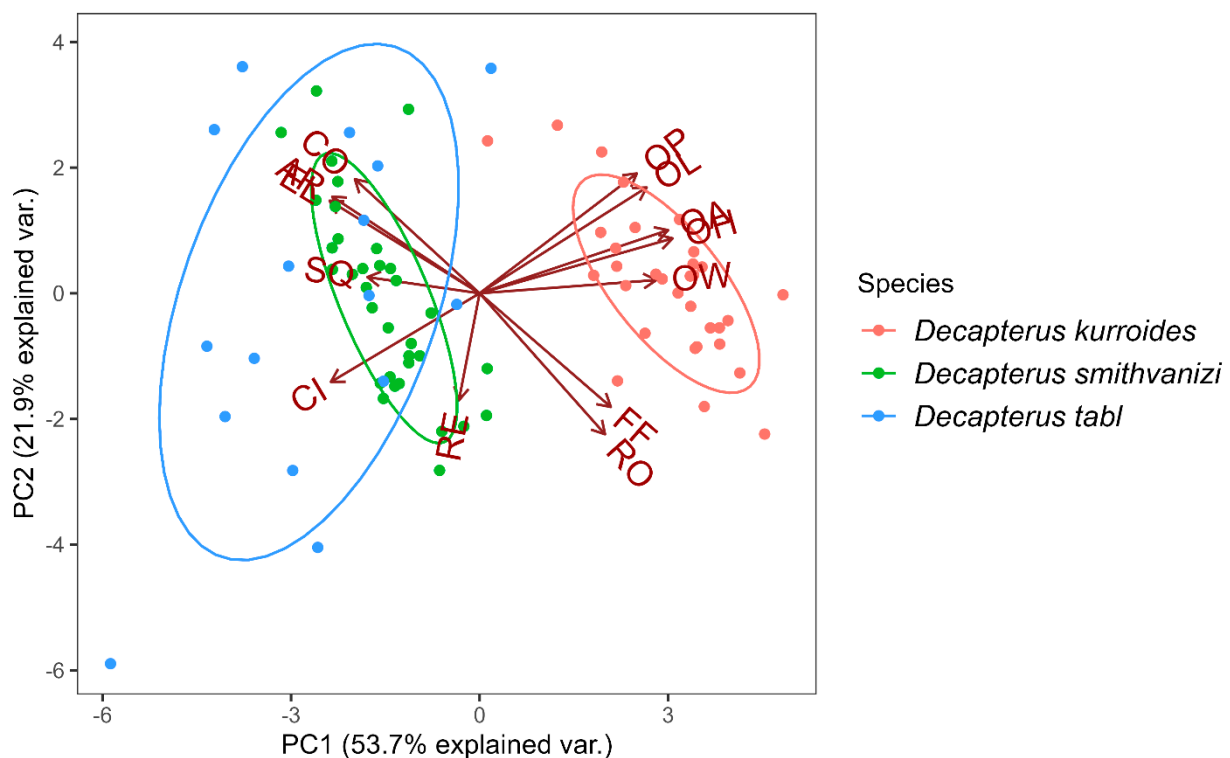


**Figure 4.** Principal Component Analysis (PCA) plot of size- and shape-related otolith indices (letters at vector ends) from the three redfin *Decapterus* species from the Sulu Sea, Philippines.

### 3.2. Otolith Shape Analysis

Overall, the otoliths had lanceolated shapes whose outlines were virtually identical (see Figure 5), but wavelet coefficients have shown statistically significant differences ( $p < 0.001$ ) in the mean shapes of the otoliths and that the coefficients were able to separate the species from each other (Figure 6). Major variations between species were seen on how pronounced the antirostrum were in Figure 5, and it was well-defined in *Decapterus tabl* (also shown in Figure 3). In addition, the posterior margin of *D. kurroides* otoliths appeared



to be more rounded than the other two species. Furthermore, the degree of dentation along the dorsal margin was less in *D. kurroides*.

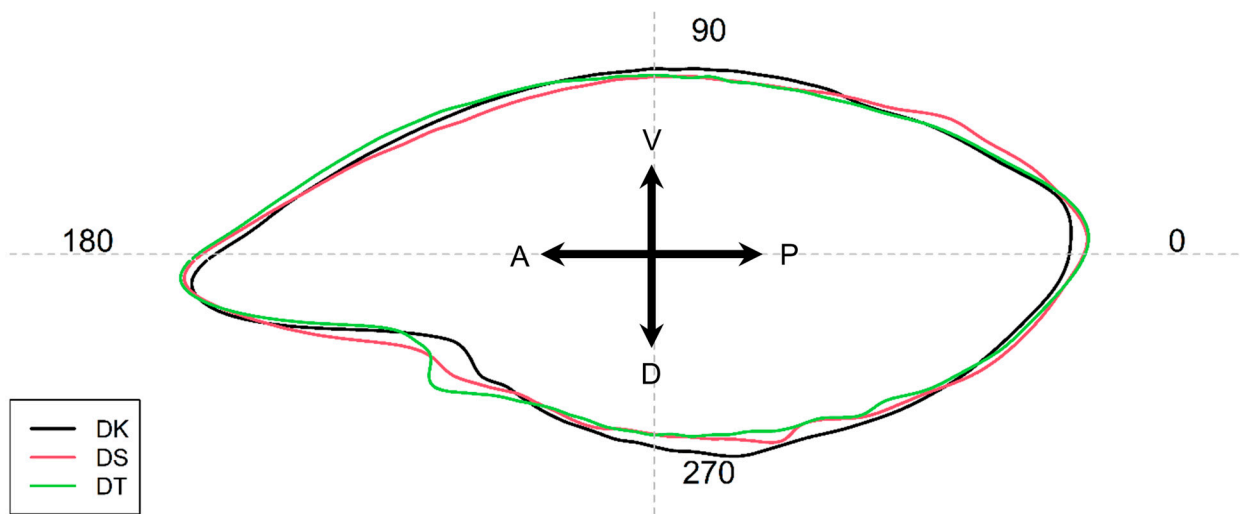


**Figure 5.** Mean otolith shapes of *Decapterus kurroides* (DK), *D. smithvanizi* (DS), and *D. tabl* (DT) based on wavelet reconstruction, extracted using the “detect.outline” function of ShapeR. Crossmap shows the position of the otolith, as in Figure 3.

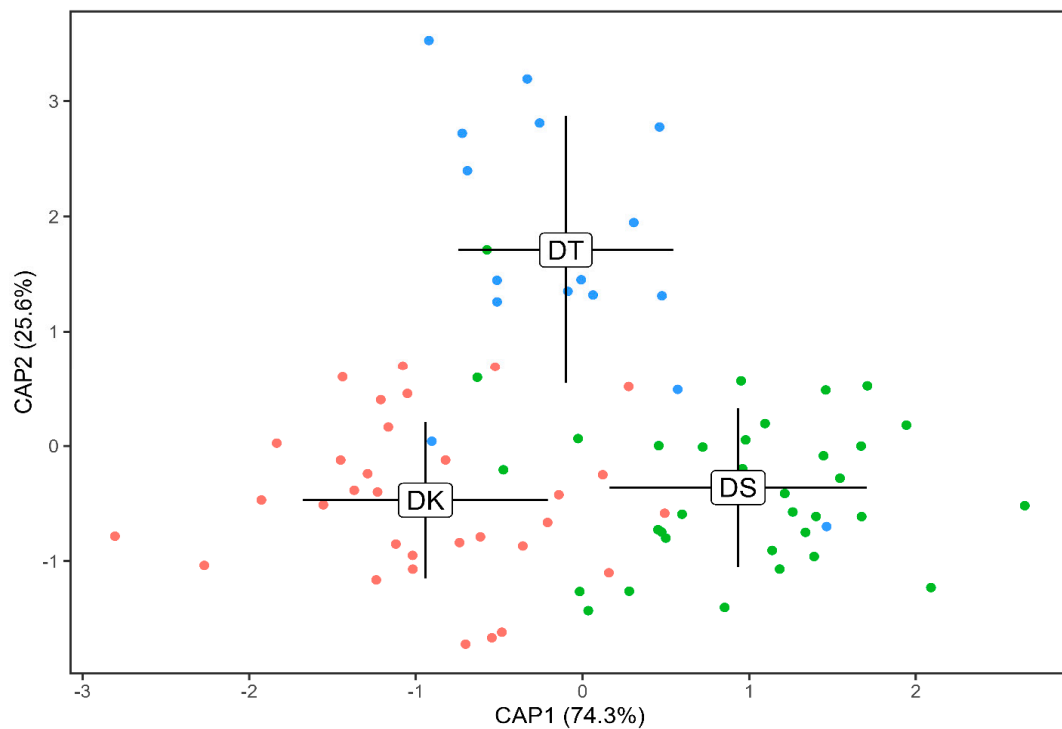


**Figure 6.** Plot showing mean otolith shapes of the three redfin *Decapterus* species from Sulu Sea, Philippines, using canonical analysis of principal coordinates (CAP) with the wavelet coefficients. Labels represent species and the mean canonical values, while surrounding points denote each individual fish of the same species (red—DK, green—DS, blue—DT). DK—*Decapterus kurroides*; DS—*D. smithvanizi*; DT—*D. tabl*. Lines surrounding the labels are the standard deviations (mean  $\pm$  SD) in both CAP1 and CAP2.

Regions of marked differences among the three species are highlighted using the mean and standard deviation as well as intraclass correlations. These were evident along the

regions 0–20°, 55–80° (postrostrum to ventral), 130–230°, 230–270° (rostrum to dorsal), and 270–340°, which are also evident in Figures 3 and 5.

#### 4. Discussion

This study explored the use of otolith shape and morphometric indices as tools to delineate the redbfin *Decapterus* species from the Sulu Sea, Philippines, namely, *Decapterus kurroides*, *D. smithvanizi*, and *D. tabl*. The results have shown that the otoliths of the three redbfin *Decapterus* species varied. The largest variation was caused by the size-related morphometric indices, OW, OL, OH, OA, and OP, which separated *Decapterus kurroides* from the overlapping *D. smithvanizi* and *D. tabl*. This divergence was also clear along the rostrum, dorsal margin, and postrostrum of the generated otolith outlines (Figure 5), which was supported by its significantly higher values for OH (size-related index) and RO (shape-related index) compared to the other two species. The shape of the rostrum and postrostrum has also shown an evident divergence by *D. kurroides* from the other two species, which also had comparable values for mean ellipticity (*D. kurroides* =  $0.378 \pm 0.02$ ; *D. smithvanizi* =  $0.404 \pm 0.02$ ; *D. tabl* =  $0.406 \pm 0.01$ ), meaning the *D. kurroides* otoliths are less elliptic or less oblong in shape.

The observed morphometric and shape differences between the otoliths of the three redbfin *Decapterus* used in this study support the specificity of otolith shape to species [13,14]. Otoliths are known to exhibit inter- and intraspecific variations due to environmental and genetic factors. Among these, according to Sadighzadeh et al. [53], genetic differences should have the greatest influence in otolith morphology. The results from this study suggest a greater genetic difference of *D. kurroides* from the other two species.

While *D. kurroides*, *D. smithvanizi*, and *D. tabl* reside in a homologous basin and are commonly integrated in fish catch, their vertical distribution is different. A report from Smith-Vaniz [54] indicated that *D. kurroides* dwell within 150–300 m depths, while *D. tabl* was reported to reach depths of 7–550 m [55], usually 150–220 m [56]. Both species are within the epipelagic to mesopelagic zone. There is currently no data indicating the depth range of *D. smithvanizi*. In FishBase, it is listed as demersal, but it can be assumed to be up to 200 m or along the neritic region, as they are also captured with purse seines, ring nets, and handlines along with *D. kurroides* and *D. tabl* in nearshore areas. The interspecific differences in the otoliths of the three redbfin *Decapterus* species used in this study reflects the differences in their depth range and distribution. Deeper waters equate to higher water pressures. According to Tuset et al. [57] and Bani et al. [58], fish that live in greater depths are expected to have larger otoliths. On the contrary, Correia et al. [59] reported that changing hydrostatic pressure does not affect otolith development in early *Oreochromis niloticus* (Linnaeus, 1758) juveniles under constant temperature and salinity.

Food and nutrient quality and availability are also among the factors that influence fish growth and, hence, otolith development [17,31,60–62]. The consequences of these will be seen in variations in the shape and morphology of otoliths. The shared common habitat among the three redbfin species of *Decapterus* suggests that available prey items and nutrients may be congruent. However, studies on their food preferences will provide more a concrete basis to support this hypothesis.

In this study, we have provided additional inputs on the diversity of structures that can be used to delineate species that closely resemble each other, such as the redbfin species. These species are harvested in various parts of the country but are treated as one species in fisheries statistics reports. One of the possible reasons is that the visual differences between the species are very minimal, especially in lower size-length classes. It is for the same reason that fishers do not segregate them in catches even until it reaches the market, because sorting would add up to the time consumed before the catches reach the target markets and consumers. However, this poses threats on the populations of these species. Roundscads, in general, are among the commercially important small pelagic fish in the Philippines and are among the top commodities in the annual volume of fisheries production. However, as in other species, data on the dynamics of these species' populations are scarce, so there is

no basis for implementation of management interventions, such as catch size and volume limits. It is also important to note that, among the three redfin species investigated, *D. tabl* is the least frequently caught; hence the low number of samples collected for this study. Treating the redfin group as a single species means that we may be fishing down fish populations while unconsciously depleting one or more of these species. Since fisheries statistics treat them as one, there is no data that could support or prove that the former statement may have taken place in the past.

This study corroborated the results of previous works and has shown the potential of using otolith shape and morphometric analyses in giving data on markers that can separate the redfin species of the genus *Decapterus*. This was specifically effective for separating *D. kurroides* from the other two species. For *D. smithvanizi* and *D. tabl*, the otoliths differed in shape but not with size- and shape-related morphometric indices. The fact that shape analysis has shown a high visual similarity between the *D. smithvanizi* and *D. tabl* otoliths shows the current limitations of the interspecific variability that otolith shape and morphometrics can reveal. It might be that, for these two species, genetics will be the most effective separator. However, the addition of more variables in morphometric analyses, such as microstructures, can be explored to investigate the most intricate differences that will enable separation of these two redfin species. For now, this methodology has shown to be very effective for the delineation of phenotypic stocks, such as in Barnuevo et al. [16]. The application of the same method in other genera will further refine the current methods and will help prove its effectiveness in delineating cryptic fish species or species that have very low variability in appearance. Studies on the biology, ecology, and dynamics of the populations of redfin *Decapterus* species should be explored. These will be important in giving a deeper understanding of the interspecific variations that exist within the group, such as the morphometrics and shape of the otoliths.

## 5. Conclusions

The major findings in this study were: (1) morphometric indices (size- and shape-related) have shown positive statistical relationships with fish length; (2) size- and shape-related indices were significantly different between species; (3) size-related indices separated *Decapterus kurroides* from the other two species, which were seen to overlap; and (4) otolith shape analysis was effective in separating the redfin species of *Decapterus* from the Sulu Sea and identified regions of marked differences in the otolith outline. Therefore, this study shows that, while progress in fish taxonomy is veering towards molecular methods, otoliths still serve as cheap alternatives that can provide significant phenotypic data that can be used to separate species and populations. Otoliths present relevant biological fish data with less investment in time and financial resources compared to molecular methods, which will be the ultimate confirmatory method. Future studies on the otoliths of the same group should consider integrating intraspecific variations that may occur in these species (e.g., ear-side effects, influences of sex, life history, etc.). Moreover, starting studies on the redfin *Decapterus* species' biology, ecology, and population dynamics will be helpful in explaining these differences.

**Author Contributions:** Conceptualization: R.P.B., C.J.C.M. and K.D.E.B.; Methodology: C.J.C.M., K.D.E.B., J.K.S.C., E.S.D.J. and R.A.C.-B.; Software: C.J.C.M. and K.D.E.B.; Validation: R.P.B., S.D.P.L. and E.S.D.J.; Formal analysis: C.J.C.M., K.D.E.B. and J.K.S.C.; Investigation: C.J.C.M., K.D.E.B., J.K.S.C. and E.S.D.J.; Data curation: C.J.C.M., K.D.E.B., J.K.S.C. and S.D.P.L.; Writing—original draft: C.J.C.M. and K.D.E.B.; Writing—review and editing: C.J.C.M., K.D.E.B., E.S.D.J., R.A.C.-B., J.K.S.C., S.D.P.L. and R.P.B.; Visualization: C.J.C.M. and K.D.E.B.; Supervision: S.D.P.L. and R.P.B.; Project administration: S.D.P.L. and R.P.B.; Funding acquisition: R.P.B. All authors have read and agreed to the published version of the manuscript.

**Funding:** This research was funded by Emerging Interdisciplinary Research (EIDR) Program of the University of the Philippines Office of the Vice President for Academic Affairs (UP-OVPAA) (OVPAE-EIDR-C08-011-R) and the University of the Philippines Visayas Office of the Vice Chancellor for research and Extension (UPV-OVCRE) (SP20-13).

**Institutional Review Board Statement:** By virtue of the Philippines' Department of Agriculture (DA) Administrative Order (AO) No. 40 (s. 1999), the Institutional Animal Care and Use Committee (IACUC) of the Animal Care and Use Program (ACUP) was thereby obligated to approve and certify experiments involving live animals. In this study, non-live fishes purchased from fish landing sites were used as test animals. As certified by the Institutional Animal Care and Use Committee (IACUC) of the University of the Philippines Visayas last 1 December 2022, detailed evaluation was not necessary.

**Data Availability Statement:** The raw data which supports this study are available from the corresponding author at reasonable request.

**Acknowledgments:** Persons who were of great help during sample collection, data processing, and expert consultations are hereby acknowledged. UPV-OVCRE is also hereby acknowledged for the APC support grant. Special thanks to Brenna Mei M. Concolis for the help in navigating through the complexities of R programming.

**Conflicts of Interest:** The authors declare no conflict of interest.

## References

1. Popper, A.N.; Ramcharitar, J.; Campana, S.E. Why otoliths? Insights from inner ear physiology and fisheries biology. *Mar. Freshw. Res.* **2005**, *56*, 497–504. [CrossRef]
2. Poznar, M.; Stolarski, J.; Sikora, A.; Mazur, M.; Olesiak-Bańska, J.; Brach, K.; Ozyhar, A.; Dobryszycycki, P. Fish otolith matrix macromolecule-64 (OMM-64) and its role in Calcium Carbonate Biomineralization. *Cryst. Growth Des.* **2020**, *9*, 5808–5819. [CrossRef]
3. Edmonds, J.S.; Steckis, R.A.; Moran, M.J.; Caputi, N.; Morita, M. Stock delineation of pink snapper *Pagrus auratus* and tailor *Pomatomus saltatrix* from Western Australia by analysis of stable isotope and strontium/calcium ratios in otolith carbonate. *J. Fish Biol.* **1999**, *55*, 243–259. [CrossRef]
4. Ovenden, J.R.; Lloyd, J.; Newman, S.J.; Keenan, C.P.; Slater, L.S. Spatial genetic subdivision between northern Australian and southeast Asian populations of *Pristipomoides multidens*: A tropical marine fish species. *Fish. Res.* **2002**, *59*, 57–69. [CrossRef]
5. Horne, J.B.; Momigliano, P.; Welch, D.J.; Newman, S.J.; van Herwerden, L. Searching for common threads in threadfins: Phylogeography of Australian polynemids in space and time. *Mar. Ecol. Prog. Ser.* **2012**, *449*, 263–276. [CrossRef]
6. Izzo, C.; Gillanders, B.M.; Ward, T.M. *Movement Patterns and Stock Structure of Australian Sardine (Sardinops sagax) off South Australia and the East Coast: Implications for Future Stock Assessment and Management. Final Report to the Fisheries Research and Development Corporation*; South Australian Research and Development Institute: West Beach, SA, USA, 2012; pp. 86–87. Available online: [https://www.fish.gov.au/Archived-Reports/2014/Documents/Izzo\\_et\\_al\\_2012.pdf](https://www.fish.gov.au/Archived-Reports/2014/Documents/Izzo_et_al_2012.pdf) (accessed on 11 October 2022).
7. Mackenzie, K.; Abaunza, P. Parasites as biological tags. In *Stock Identification Methods: Applications in Fishery Science*; Cadrin, S.X., Friedland, K.D., Waldman, J.R., Eds.; Elsevier Academic Press: San Diego, CA, USA, 2005; pp. 211–226.
8. Friedland, K.D.; Cadrin, S.X. Analyses of calcified structures: Texture and spacing patterns. In *Stock Identification Methods: Applications in Fishery Science*; Cadrin, S.X., Friedland, K.D., Waldman, J.R., Eds.; Elsevier Academic Press: San Diego, CA, USA, 2005; pp. 185–195.
9. Newman, S.J.; Steckis, R.A.; Edmonds, J.S.; Lloyd, J. Stock structure of the goldband snapper, *Pristipomoides multidens* (Pisces: Lutjanidae) from the waters of northern and western Australia by stable isotope ratio analysis of sagittal otolith carbonate. *Mar. Ecol. Prog. Ser.* **2000**, *198*, 239–247. [CrossRef]
10. Newman, S.J.; Buckworth, R.C.; Mackie, M.C.; Lewis, P.D.; Wright, I.W.; Williamson, P.C.; Bastow, T.P.; Ovenden, J.R. Spatial subdivision among assemblages of Spanish mackerel, *Scomberomorus commerson* (Pisces: Scombridae) across northern Australia: Implications for fisheries management. *Glob. Ecol. Biogeogr.* **2009**, *18*, 711–723. [CrossRef]
11. Newman, S.J.; Wright, I.W.; Rome, B.M.; Mackie, M.C.; Lewis, P.D.; Buckworth, R.C.; Ballagh, A.C.; Garrett, R.N.; Stapley, J.; Broderick, D.; et al. Stock structure of grey mackerel, *Scomberomorus semifasciatus* (Pisces: Scombridae) across northern Australia, based on otolith stable isotope chemistry. *Environ. Biol. Fishes* **2010**, *89*, 357–367. [CrossRef]
12. Begg, G.A. Life history parameters. In *Stock Identification Methods: Applications in Fishery Science*; Cadrin, S.X., Friedland, K.D., Waldman, J.R., Eds.; Elsevier Academic Press: San Diego, CA, USA, 2005; pp. 119–150.
13. Campana, S.E. Photographic atlas of fish otolith of the northwest Atlantic Ocean. In *Canadian Special Publication of Fisheries and Aquatic Sciences 133*; NCR, Research Press: Ottawa, ON, Canada, 2004; p. 284.
14. Tuset, V.M.; Lombarte, A.; Assis, C.A. Otolith atlas for the western Mediterranean, north, and central eastern Atlantic. *Sci. Mar.* **2008**, *72*, 7–198. [CrossRef]

15. Lombarte, A.; Castellón, A. Interspecific and intraspecific otolith variability in the genus *Merluccius* as determined by image analysis. *Can. J. Zool.* **1991**, *69*, 2442–2449. [[CrossRef](#)]
16. Barnuevo, K.D.E.; Morales, C.J.C.; Calizo, J.K.S.; Delloro, E.S., Jr.; Añasco, C.P.; Babaran, R.P.; Lumayno, S.D.P. Distinct stocks of the redbtail scad *Decapterus kurroides* Bleeker, 1855 (Perciformes: Carangidae) from the northern Sulu and Southern Sibuyan Seas, Philippines revealed from otolith morphometry and shape analysis. *Fishes* **2023**, *8*, 12. [[CrossRef](#)]
17. Mille, T.; Mahé, K.; Villanueva, M.C.; De Pontual, H.; Ernande, B. Sagittal otolith morphogenesis asymmetry in marine fishes. *J. Fish Biol.* **2015**, *87*, 646–663. [[CrossRef](#)]
18. Kondaş, S.; Bostanci, D.; Yedier, S.; Kurucu, G.; Polat, N. Investigation of fluctuating asymmetry in the four otolith characters of *Merlangius merlangus* collected from middle Black Sea. *Turk. J. Marit. Marine Sci.* **2018**, *4*, 128–138. Available online: <https://dergipark.org.tr/en/pub/trjmms/issue/40277/485515> (accessed on 13 January 2023).
19. Mejri, M.; Trojette, M.; Jmil, I.; Ben Faleh, A.; Chalh, A.; Quignard, J.-P.; Trabelsi, M. Fluctuating asymmetry in the otolith shape, length, width and area of *Pagellus erythrinus* collected from the Gulf of Tunis. *Cah. Biol. Mar.* **2020**, *61*, 1–7. [[CrossRef](#)]
20. Geladakis, G.; Somarakis, S.; Koumoundouros, G. Differences in otolith shape and fluctuating asymmetry between reared and wild gilthead seabream (*Sparus aurata* Linnaeus, 1758). *J. Fish Biol.* **2021**, *98*, 277–286. [[CrossRef](#)] [[PubMed](#)]
21. Jawad, L.A.; Qasim, A.M.; Al-Faiz, N.A. Bilateral asymmetry in size of otolith of *Otolithes ruber* (Bloch and Schneider, 1801) collected from the marine waters of Iraq. *Mar. Poll. Bull.* **2021**, *165*, 112110. [[CrossRef](#)]
22. Mahé, K.; MacKenzie, K.; Ider, D.; Massaro, A.; Hamed, O.; Jurado-Ruzafa, A.; Gonçalves, P.; Anastasopoulou, A.; Jadaud, A.; Mytilineou, C.; et al. Directional bilateral asymmetry in fish otolith: Potential tool to evaluate stock boundaries? *Symmetry* **2021**, *13*, 987. [[CrossRef](#)]
23. Vignon, M.; Morat, F. Environmental and genetic determinant of otolith shape revealed by a non-indigenous tropical fish. *Mar. Ecol. Prog. Ser.* **2010**, *411*, 231–241. [[CrossRef](#)]
24. Campana, S.E.; Neilson, J.D. Microstructure of fish otoliths. *Can. J. Fish. Aquat. Sci.* **1985**, *42*, 1014–1032. [[CrossRef](#)]
25. Mosegaard, H.; Svedäng, H.; Taberman, K. Uncoupling of somatic and otolith growth rates in Arctic Char (*Salvelinus alpinus*) as an effect of differences in temperature response. *Can. J. Fish. Aquat. Sci.* **1988**, *45*, 1514–1524. [[CrossRef](#)]
26. Libungan, L.A.; Oskarsson, G.J.; Slotte, A.; Jacobsen, J.A.; Palsson, S. Otolith shape: A population marker for Atlantic herring *Clupea herengus*. *J. Fish Biol.* **2015**, *86*, 1377–1395. [[CrossRef](#)] [[PubMed](#)]
27. Berg, F.; Almeland, O.W.; Skadal, J.; Slotte, A.; Andersson, L.; Folkvord, A. Genetic factors have a major effect on growth, number of vertebrae and otolith shape in Atlantic Herring (*Clupea harengus*). *PLoS ONE* **2018**, *13*, e0190995. [[CrossRef](#)] [[PubMed](#)]
28. Capoccioni, F.; Costa, C.; Aguzzi, J.; Menesatti, P.; Lombarte, A.; Ciccotti, E. Ontogenetic and environmental effects on otolith shape variability in three Mediterranean European eel (*Anguilla anguilla* L.) local stocks. *J. Exp. Mar. Biol. Ecol.* **2011**, *397*, 1–7. [[CrossRef](#)]
29. Curcio, N.; Tombari, A.; Capitanio, F. Otolith morphology and feeding ecology of an Antarctic nototheniid, *Lepidonotothen larseni*. *Antarct. Sci.* **2013**, *26*, 124–132. [[CrossRef](#)]
30. Tuset, V.M.; Imondi, R.; Aguado, G.; Otero-Ferrer, J.L.; Santschi, L.; Lombarte, A.; Love, M. Otolith patterns of rockfishes from the northeastern Pacific. *J. Morphol.* **2015**, *276*, 458–469. [[CrossRef](#)]
31. Mille, T.; Mahé, K.; Cachera, M.; Villanueva, M.C.; de Pontual, H.; Ernande, B. Diet is correlated with otolith shape in marine fish. *Mar. Ecol. Prog. Ser.* **2016**, *555*, 167–184. [[CrossRef](#)]
32. Cardinale, M.; Doering-Arjes, P.; Kastowsky, M.; Mosegaard, H. Effects of sex, stock, and environment on the shape of known-age Atlantic cod (*Gadus morhua*) otoliths. *Can. J. Fish. Aquat. Sci.* **2004**, *61*, 158–167. [[CrossRef](#)]
33. Santos, M.D. Seasonality of commercially important pelagic fishes in the Philippines: Overfishing or climate change? In Proceedings of the International Workshop on Climate and Oceanic Fisheries, Rarotonga, Cook Islands, 3–5 October 2011.
34. Philippine Statistics Authority. *Fisheries Statistics of the Philippines (2018–2020)*; Philippine Statistics Authority: Quezon City, Philippines, 2020; p. 320.
35. Kimura, S.; Katahira, K.; Kuriwa, K. The red-fin *Decapterus* group (Perciformes: Carangidae) with the description of a new species, *Decapterus smithvanizi*. *Ichthyol. Res.* **2013**, *60*, 363–379. [[CrossRef](#)]
36. Fricke, R.; Eschmeyer, W.N.; Van der Laan, R. (Eds.) *Eschmeyer's Catalog of Fishes: Genera, Species, References*. Electronic Version. 2022. Available online: <http://researcharchive.calacademy.org/research/ichthyology/catalog/fishcatmain.asp> (accessed on 14 October 2022).
37. Narido, C.I.; Palla, H.P.; Argente, F.A.T.; Geraldino, P.J.L. Population dynamics and fishery of Roughear scad *Decapterus tabl* Berry 1968 (Perciformes: Carangidae) in Camotes Sea, Central Philippines. *Asian Fish. Sci.* **2016**, *29*, 14–27. [[CrossRef](#)]
38. Kimura, S. Family Carangidae: *Decapterus tabl*. In *Commercial and Bycatch Market Fishes of Panay Island, Republic of the Philippines*; Motomura, H., Alama, U.B., Muto, N., Babaran, R.P., Ishikawa, S., Eds.; Kagoshima University Museum, Kagoshima, University of the Philippines Visayas, Iloilo, and Research Institute for Humanities and Nature: Kyoto, Japan, 2017; p. 115.
39. Motomura, H.; Alama, U.B.; Muto, N.; Babaran, R.P.; Ishikawa, S. *Commercial and Bycatch Market Fishes of Panay Island, Republic of the Philippines*; Kagoshima University Museum, Kagoshima, University of the Philippines Visayas, Iloilo, and Research Institute for Humanities and Nature: Kyoto, Japan, 2017; p. 246.
40. Smith-Vaniz, W.F.; Carpenter, K.E.; Jiddawi, N.; Borsa, P.; Obota, C.; Yahya, S. *Decapterus smithvanizi*. *IUCN Red List. Threat. Species* **2018**, e.T123424845A123494632. [[CrossRef](#)]

41. Delloro, E.S., Jr.; Babaran, R.P.; Gaje, A.C.; Cambroner, P.T.; Alama, U.B.; Motomura, H. First record of slender scad, *Decapterus smithvanizi* (Actinopterygii: Perciformes: Carangidae) from the Philippines. *Acta Ichthyol. Piscat.* **2021**, *51*, 233–239. [CrossRef]
42. Osman, Y.; Mahe, K.; El-Mahdy, S.; Mohammad, A.; Mehanna, S. Relationship between body and otolith morphological characteristics of sabre squirrelfish (*Sargocentron spiniferum*) from the southern Red Sea: Difference between right and left otoliths. *Oceans* **2021**, *2*, 624–633. [CrossRef]
43. Libungan, L.A.; Pálsson, S. ShapeR: An R package to study otolith shape variation among fish populations. *PLoS ONE* **2015**, *10*, e0121102. [CrossRef]
44. RStudio Team. *RStudio: Integrated Development for R*; RStudio, PBC: Boston, MA, USA, 2020; Available online: <http://www.rstudio.com/> (accessed on 1 December 2022).
45. Oksanen, J.; Blanchet, F.G.; Kindt, R.; Legendre, P.; Minchin, P.R.; O'Hara, R.B.; Simpson, G.L.; Solymos, P.; Stevens, M.H.H.; Wagner, H. *Vegan: Community Ecology Package*, Version 2.0-7. R Package. 2013. Available online: <https://CRAN.R-project.org/package=vegan/> (accessed on 1 December 2022).
46. Wickham, H. *Ggplot2: Elegant Graphics for Data Analysis*, 2nd ed.; Springer: Cham, Switzerland, 2016.
47. The Jamovi Project. *Jamovi (Version 2.3.18)* [Computer Software]. 2022. Available online: <https://www.jamovi.org> (accessed on 1 December 2022).
48. Zischke, M.T.; Litherland, L.; Tilyard, B.R.; Stratford, N.J.; Jones, E.L.; Wang, Y.G. Otolith morphology of four mackerel species (*Scomberomorus* spp.) in Australia: Species differentiation and prediction for fisheries monitoring and assessment. *Fish. Res.* **2016**, *176*, 39–47. [CrossRef]
49. Tuset, V.M.; Olivar, M.P.; Otero-Ferrer, J.L.; López-Pérez, C.; Hulley, P.A.; Lombarte, A. Morpho-functional diversity in *Diaphus* spp. (Pisces: Myctophidae) from the Central Atlantic Ocean: Ecological and evolutionary implications. *Deep Sea Res.* **2018**, *1138*, 46–59. [CrossRef]
50. Deepa, K.P.; Aneesh Kumar, K.V.; Kottanis, O.; Nikki, R.; Bineesh, K.K.; Hashim, M.; Saravanane, N.; Sudhakar, M. Population variations of Opal fish, *Bembrops caudimacula* Steindachner, 1876 from Arabian Sea and Andaman Sea: Evidence from otolith morphometry. *Reg. Stud. Mar. Sci.* **2019**, *25*, 100466. [CrossRef]
51. Leonart, J.; Salat, J.; Torres, G.J. 2000. Removing allometric effects of body size in morphological analysis. *J. Theor. Biol.* **2000**, *205*, 85–93. [CrossRef]
52. Elliott, N.G.; Haskard, K.; Koslow, J.A. Morphometric analysis of orange roughy (*Hoplostethus atlanticus*) off the continental slope of Southern Australia. *J. Fish. Biol.* **1995**, *46*, 202–220. [CrossRef]
53. Sadighzadeh, Z.; Valinassab, T.; Vosugi, G.; Montallebi, A.A.; Fatemi, M.R.; Lombarte, A.; Tuset, V.M. use of otolith shape for stock identification of John's snapper, *Lutjanus johnii* (Pisces: Lutjanidae), from Persian Gulf and the Oman Sea. *Fish. Res.* **2014**, *155*, 59–63. [CrossRef]
54. Smith-Vaniz, W.F. Carangidae. In *Smith's Sea Fishes*; Smith, M.M., Heemstra, P.C., Eds.; Springer: Berlin, Germany, 1986; pp. 638–661.
55. de Figueiredo, J.L.; dos Santos, A.P.; Yamaguti, N.; Bernardes, R.A.; Del Bianco Rossi-Wongtschowski, C.L. *Peixes da Zona Econômica Exclusiva da Região Sudeste-Sul do Brasil: Levantamento com Rede de Meia-Água*; Editora da Universidade de São Paulo, Imprensa Oficial do Estado: São-Paulo, Brazil, 2002; p. 242.
56. Cervignón, F.; Cipriani, R.; Fischer, W.; Garibaldi, L.; Hendrickx, M.; Lemus, A.J.; Márquez, R.; Putiers, J.M.; Robaina, G.; Rodríguez, B. *Fichas Fao de Identificación de Especies Para Los Fines de la Pesca. Guía de Campo de Las Especies Comerciales Marinas Y de Aguas Salobres de la Costa Septentrional de Sur América*; FAO: Rome, Italy, 1992; p. 513.
57. Tuset, V.M.; Lombarte, A.; Gonzalez, J.A.; Pertusa, J.F.; Lorente, M. Comparative morphology of the sagittal otolith in *Serranus* spp. *J. Fish Biol.* **2003**, *63*, 1491–1504. [CrossRef]
58. Bani, A.; Poursaeid, S.; Tuset, V. Comparative morphology of the sagittal otolith in three species of south Caspian gobies. *J. Fish Biol.* **2013**, *82*, 1321–1332. [CrossRef]
59. Correia, A.T.; Coimbra, A.M.; Damasceino-Oliveira, A. Effect of hydrostatic pressure on otolith growth of early juveniles of Nile Tilapia *Oreochromis niloticus*. *J. Fish. Biol.* **2012**, *81*, 329–334. [CrossRef] [PubMed]
60. Gagliano, M.; McCormick, M.I. Feeding history influences otolith shape in tropical fish. *Mar. Ecol. Prog. Ser.* **2004**, *278*, 291–296. [CrossRef]
61. Hüsey, K. Otolith shape in juvenile cod (*Gadus morhua*): Ontogenetic and environmental effects. *J. Exp. Mar. Biol. Ecol.* **2008**, *364*, 35–41. [CrossRef]
62. Qiao, J.; Zhu, R.; Chen, K.; Zhang, D.; Yan, Y.; He, D. Comparative otolith morphology of two morphs of *Schizopygopsis thermalis* Herzenstein 1891 (Pisces, Cyprinidae) in a Headwater Lake on the Qunghai-Tibet Plateau. *Fishes* **2022**, *7*, 99. [CrossRef]

**Disclaimer/Publisher's Note:** The statements, opinions and data contained in all publications are solely those of the individual author(s) and contributor(s) and not of MDPI and/or the editor(s). MDPI and/or the editor(s) disclaim responsibility for any injury to people or property resulting from any ideas, methods, instructions or products referred to in the content.